Structure, Bonding, and Relative Stability of the Ground and Low-Lying Electronic States of CuO_2. The role of exact exchange.

Mireia Güell,[1] Josep M. Luis,[1] Luís Rodríguez-Santiago,[2]
Mariona Sodupe[2] and Miquel Solà[1*]

[1] *Institut de Química Computacional and Departament de Química, Universitat de Girona, Campus de Montilivi E-17071, Girona, Catalonia, Spain.*
[2] *Departament de Química, Universitat Autònoma de Barcelona, Bellaterra, E-08193 Barcelona, Spain.*

Corresponding author e-mail address: miquel.sola@udg.edu

Title running head: Low-Lying Electronic States of CuO_2

ABSTRACT

The C_{2v} and C_s ground and low-lying states of doublet CuO_2 are examined for a series of different density functionals (pure, hybrid, and meta-hybrid) and CCSD(T) methods. The effect of changing the B3LYP functional a_o parameter is also explored. CCSD(T) results at the complete basis set limit show that the relative stability of the different electronic states is $^2A_2(C_{2v}) < {}^2A''(C_s) < {}^2B_2(C_{2v}) < {}^2A'(C_s) << {}^2A_1(C_{2v}) < {}^2B_1(C_{2v})$. Unlike CCSD(T), all DFT methods analyzed in this work erroneously predict the end-on ^2A" state as the ground state for CuO_2 irrespective of the type of functional and percentage of Hartree-Fock (exact) exchange included in the B3LYP-like functional. Among the different functionals tested, B3LYP gives the best geometries and relative energies for the different electronic states when compared to CCSD(T) results. As to the effect of the a_o parameter is concerned, it is found that the B3LYP-like functional yielding better geometries contains 20% of exact exchange, although somewhat unexpectedly, for relative energies the B3LYP-like functional with a larger contribution of exact exchange (90%) is the one giving the smaller standard deviation.

INTRODUCTION

Copper, despite its toxicity in pure form, is fundamental for the activity of many enzymes, which are important in oxygen transport and insertion, electron transfer, redox processes, and so forth.[1-5] One of the most important enzymes in humans that contains copper in the active site is the superoxide dismutase (SOD).[6] This enzyme provides cellular defense against the oxidative stress by catalyzing $O_2^{\cdot -}$ disproportionation into the less toxic dioxygen and hydrogen peroxide:

$$2\ O_2^{\cdot -} + 2H^+ \rightarrow O_2 + H_2O_2 \qquad (1)$$

The copper site is at the heart of the enzymatic active site of the SOD protein. The catalysis is a two-step process: one molecule of superoxide first reduces Cu^{2+} to form dioxygen and then a second molecule of $O_2^{\cdot -}$ reoxidizes Cu^+ to form hydrogen peroxide (See Figure 1).[7,8]

Figure 1, here

In order to study theoretically the mechanism for the toxic superoxide radical disproportionation by SOD, it is necessary to employ methods that describe correctly the interaction between copper ions (Cu^+ and Cu^{2+}) and the superoxide radical ($O_2^{\cdot -}$). Most of the articles that study catalytic mechanisms computationally in enzymes use density functional theory (DFT) methods.[9-12] DFT is the usual method of choice for studies of enzymatic or organometallic catalytic reaction mechanisms because the current hybrids or meta-GGA functionals provide, in general, similar or even better results on geometries and relative energies compared to correlated *ab initio* calculations such as MP2 while using less computer time.[9-12] Unfortunately, however, this is not always the case. For instance, recently, some of us showed that many DFT methods fail to predict the correct ground electronic state of Cu^{2+}-H_2O.[13] This is due to the fact that, in certain electronic states, there is an important charge and spin delocalization. These situations, as for two center-three electron (2c-3e) bond systems,[14-16] have been shown to be overstabilized by most pure density functionals. For this reason, it was also found that the relative stability of the different electronic states in Cu^{2+}-H_2O strongly depends on the degree of mixing of exact HF and DFT exchange functional.[13] Among the

different functionals tested in that work,[13] the BHandHLYP functional was found to be the one that provides better results compared to CCSD(T).

Before starting the investigation of any reaction mechanism involving Cu^{+}- or Cu^{2+}-$O_2^{\cdot-}$ species with DFT methods, it is convenient to make a detailed study of the performance of different DFT methods for the description of the geometry and energetics of the ground and low-lying states of CuO_2 and CuO_2^{+}. This is the main goal pursued by the present paper. Hartree-Fock (HF) and coupled cluster with single and double excitations[17] with the perturbation theory to include the effect of triple excitations[18] (CCSD(T)) calculations with a complete basis set (CBS) extrapolation will be also carried out to get reference values to which our DFT results can be compared. Preliminary calculations of the singlet and triplet CuO_2^{+} species show that, qualitatively, the DFT relative energies of the ground and low-lying electronic states follow the same trends as those provided by the CCSD(T) method. For this reason, the present paper is focused on the capability of DFT to provide the right energetic order and geometry (end-on C_s or side-on C_{2v}, Figure 2) of the ground and low-lying states of the doublet CuO_2. Quartet states of CuO_2 have not been considered here because they are basically van der Waals complexes far less stable than doublet states.[19,20] For doublet CuO_2 species, we will also analyze the effect of changing the amount of HF exchange included in the B3LYP functional. Let us mention here that several benchmarks on the performance of different functionals for the study of inorganometallic and organometallic complexes are available in the literature.[21-27]

Figure 2, here

The CuO_2 species has been extensively studied both experimentally and theoretically. It is known that a $Cu(O_2)$ (hereafter referred as CuO_2) weakly bound complex is formed when Cu reacts with O_2 in rare-gas matrices.[20,28-33] The linear OCuO dioxide that is formed after irradiation in the ultraviolet[34] is more strongly bound but it is less stable and will not be studied in the present work. Interestingly, the global minima on the M + O_2 potential energy surfaces (PESs) of all first-row transition metals correspond to the dioxide structure, the only exception being the CuO_2 with a superoxide structure.[35] Mitchell has determined that the bond dissociation in the ground state angular CuO_2 is 15 ± 5 kcal mol^{-1}.[36] On the other hand, EPR experiments[29-31]

indicate two magnetically inequivalent oxygen atoms and this has been interpreted in terms of an end-on C_s coordination (see Figure 2) for the ground state of CuO_2. HF[37] and DFT(B3LYP)[19,20,38] studies reinforce this result by showing that the end-on C_s structure is about 10 kcal mol^{-1} more stable than the side-on C_{2v} species. However, at the ab initio correlated level (MRCI,[39] CASPT2,[37] and CCSD(T)[40,41] calculations) the side-on structure is found to be the ground state, with the end-on isomer being almost isoenergetic (only about 1 kcal mol^{-1} less stable). One of us[40] attributed the difference between EPR results and theoretical predictions by high level calculations to matrix effects taking place in EPR experiments that could either change the relative stabilities or produce an external magnetic field that cause the oxygen atoms of the C_{2v} side-on structure to be magnetically inequivalent. More recent calculations by Roos et al.[37] provided further support for the larger stabilization of the C_s as compared to the C_{2v} structure in rare-gas matrices, due to its larger dipole moment.

As said before, in the present work we address the effect of varying the fraction of exact HF exchange included in hybrid B3LYP-like functional on the relative energy and geometry of the ground and low-lying states of doublet CuO_2. The effect of changing the amount of HF exchange included in the B3LYP functional in the molecular structure,[42-47] vibrational frequencies,[45,47] first-order density,[48] thermochemistry and energy barriers,[42,49-53] ionization potentials,[54] hydrogen bond infrared signature,[55] and nuclear resonance shielding constants[56] of several species has been discussed in previous works.[42,56] Furthermore, Reiher and co-workers[57] have analyzed the importance of the admixture of exact HF exchange in the functional on the relative energy between electronic states of different multiplicities. These authors have shown that high-spin states in Fe(II)-sulfur complexes are stabilized when the degree of exact HF exchange is increased and that the energy splitting between low-spin and high-spin states depends *linearly* on the coefficient of the HF exchange admixture. Because of problems with the B3LYP functional[58] for providing the spin ground-state of iron-sulfur complexes, Reiher and co-workers[57] therefore proposed to lower the amount of HF exchange in B3LYP to 15%. This reparametrized functional, called B3LYP*, was indeed shown to afford better relative energies between electronic states as compared to B3LYP, but still failed for spin-crossover systems.[59] More recently, validation studies of DFT functionals[60] have shown the excellent performance of the OPBE and OLYP[61-

[63] functionals for these spin-state splittings. These functionals will be included in our study.

Up to date, the CuO_2 molecule has been studied by DFT methods with only the B3LYP[20,38] and the PW GGA-II functionals.[19] In the present work, we will consider a wider series of functionals of different types (pure, hybrid, and meta-hybrid) as well as a set of B3LYP-like functionals with different degree of HF exchange incorporation.

METHODOLOGY

HF, CCSD(T), and DFT calculations on geometries, energies, and harmonic vibrational frequencies of the C_s $^2A''$and $^2A'$ and C_{2v} $^2A_2$, $^2B_2$, $^2A_1$, and $^2B_1$ electronic states of the doublet CuO_2 species have been performed within the unrestricted formalism using the Gaussian 03 package program[64] for the HF and DFT methods and with the Molpro 2006.1 for the CCSD(T) calculations.[65] The S^2 expectation value (for DFT, this value is obtained using a Slater determinant constructed with the Kohn-Sham orbitals as approximate wavefunction) is, with few exceptions, close to the expected 0.75 value (see Table S1). CCSD(T) calculations have been done correlating all the electrons except the 1s electrons of O and the 1s, 2s, and 2p electrons of Cu. The 6-311+G(d) basis set as implemented in the Gaussian 03 has been used for all calculations. For Cu, this basis corresponds to the (14s9p5d)/[9s5p3d] Wachters basis set[66] with the contraction scheme 611111111/51111/311 supplemented with one s, two p, and one d diffuse functions and one f polarization function.[67] Moreover, single point CCSD(T) energy calculations at the optimized CCSD(T)/6-311+G(d) geometry were carried out with the Dunning's aug-cc-pVTZ and aug-cc-pVQZ basis sets.[68] From these results we provide an estimation using the eq. (7) of reference 69 of the CCSD(T) energy extrapolated to a CBS limit. This equation has been employed to extrapolate both the HF and the correlation energy. For the two-lowest energy states, we have performed additional geometry optimizations with the Dunning's aug-cc-pVTZ and aug-cc-pVQZ basis sets.[68]

For the DFT calculations, we have used the Lee, Yang, and Parr (LYP)[70] correlation functional combined with the nonlocal hybrid Becke's three parameter exchange functional (B3).[58] The B3 method was originally formulated as:[58]

$$E_{XC} = E_X^{LSDA} + a_0\left(E_X^{exact} - E_X^{LSDA}\right) + a_x \Delta E_X^{B88} + a_c \Delta E_c^{PW91} \qquad (2)$$

The E_X^{exact}, E_X^{LSDA}, ΔE_X^{B88}, and ΔE_C^{PW91} terms are the HF exchange energy based on Kohn-Sham orbitals, the uniform electron gas exchange-correlation energy, Becke's 1988 gradient correction for exchange,[71] and the 1991 Perdew and Wang gradient correction to correlation,[72-75] respectively. Commonly, this procedure is referred to as the B3PW91 method. The coefficients a_o, a_x, and a_c were determined by Becke[58] by a linear least-squares fit to 56 experimental atomization energies, 42 ionization potentials, and 8 proton affinities. The values thus obtained were $a_o = 0.20$, $a_x = 0.72$, and $a_c = 0.81$. In the Gaussian 03[64] implementation, the expression of the B3LYP functional is similar to eq. (2) with some minor differences:[76]

$$E_{XC} = E_X^{LSDA} + a_0\left(E_X^{exact} - E_X^{LSDA}\right) + a_x \Delta E_X^{B88} + E_C^{VWN} + a_c\left(\Delta E_C^{LYP} - E_C^{VWN}\right) \qquad (3)$$

In this equation, the Perdew and Wang correlation functional originally used by Becke is replaced by the Lee-Yang-Parr (LYP)[70] one. Since the LYP functional already contains a local part and a gradient correction, one has to remove the local part to obtain a correct implementation. This can be done in an approximate way by subtracting E_C^{VWN} from ΔE_C^{LYP}. Note that in the Gaussian 03 implementation the VWN functional is the one derived by Vosko et al. from a fit to the random phase approximation[77,78] results. It is also worth noting that the set of parameters $a_o = 1.0$, $a_x = a_c = 0$ does not reproduce the HF results due to the presence of the E_C^{VWN} term in eq. (3).

Besides these functionals, others have also been tested. First, we have used the pure exchange functional OPTX[61] combined with the LYP[70] (OLYP) and PBE[62,79] (OPBE) correlation functionals as well as the pure BLYP,[71] G96LYP,[80] and mPWPW91.[81] Second, we have employed the hybrids B3LYP*,[57] which uses 15% Hartree-Fock exchange compared to the 20% used in the original B3LYP, and Becke's half-and-half method (BHandH),[82] that also makes use of eq. (3) with $a_o = 0.5$, $a_x = 0.5$ and $a_c = 0$. Finally, we have tested four meta-hybrid functionals, the M05,[83] VSXC,[84]

HCTH/407,[85] and TPSS[86] functionals. According to Zhao, Schultz, and Truhlar,[87] the BLYP, G96LYP, PBE, mPWPW91, and M05 are the most efficient functionals for the description of transition metal–ligand and transition metal–transition metal bond energies.

RESULTS AND DISCUSSION

Cu^+ is one of the two most common ions formed by copper. Its electron configuration is $4s^0 3d^{10}$ and it is a diamagnetic ion. The superoxide anion is the product of the one-electron reduction of dioxygen, which occurs widely in nature. With one unpaired electron, the superoxide ion is a free radical, and, like dioxygen, it is paramagnetic. When Cu^+ and the superoxide anion are combined, the doublet CuO_2 molecule is obtained. We have performed geometric optimizations and frequency calculations for doublet CuO_2 in different C_s and C_{2v} electronic states (Figure 2). It is worth mentioning here that previous MRSDCI calculations[39] proved that in the C_s ^2A" and ^2A' states (and therefore most likely in the C_{2v} $^2A_2$ and $^2B_2$ states, *vide infra*) the RHF configuration dominates the final wavefunction. Therefore, it is expected that the single reference based CCSD(T) method yields an accurate description of these electronic states. Indeed, the test T1[88] that provides an estimation of the importance of static correlation is never larger than 0.06 for all analyzed electronic states, except for the highest $^2B_1$ one, for which T1 is 0.11. Consequently, non-dynamical correlation may be important for this state. Note that in the $^2B_1$ electronic state metal inserts into the O_2 bond (*vide infra*).

A. CuO_2 description by the HF, CCSD(T), and standard DFT methods

Table 1 contains the optimized geometrical parameters of the ground and low-lying electronic states of CuO_2 doublet obtained with HF, BLYP, G96LYP, OLYP, OPBE, mPWPW91, B3LYP, B3LYP*, BHandH, M05, VSXC, HCTH, and TPSS and the highly correlated CCSD(T) post-HF-method using the 6-311+G(d) basis set for the C_s and C_{2v} low-lying electronic states. In Table 2, the standard deviations for the optimized geometries obtained with the different methods as compared to the CCSD(T)/6-311+G(d) results are given. Table 3 shows the relative energies obtained

with these different methods, while Table 4 contains the same relative energies computed with the CCSD(T) method theory using the aug-cc-pVTZ and aug-cc-pVQZ basis set as well as an estimation of the CCSD(T) energy extrapolated to the CBS limit at the CCSD(T)/6-311+G(d) optimized geometries. Finally, Table 5 lists the geometrical parameters and relative energies of the two lowest-energy states computed at the CCSD(T) level with the aug-cc-pVTZ and aug-cc-pVQZ basis sets together with an estimation of the CCSD(T) relative energy extrapolated to the CBS limit obtained using the CCSD(T)/aug-cc-pVQZ geometry.

Tables 1-5, here

The calculated B3LYP molecular orbitals (MOs) for the different electronic states and the qualitative MO diagram for the interaction between the Cu (^{2}S) and O_2 ($^3\Sigma_g^-$) fragments in the side-on C_{2v} CuO_2 species are given in Tables S3-S8 and Figure S1, respectively, of the supporting information. Bonding orbitals for side-on CuO_2 are located well below the HOMO, while the upper levels, which are either nonbonding or antibonding, exhibit small Cu–O_2 overlaps.[19] For the C_{2v} species, we have analyzed the lowest-lying $^2A_2$, $^2B_2$, $^2A_1$, and $^2B_1$ electronic states. The results show that in the $^2A_2$ state the singly occupied MO (SOMO) is the $2a_2$ orbital, which is an antibonding combination of the copper d_{yz} orbital with the $\pi*$ out-of-plane antibonding MO of O_2, the latter having a larger amplitude. The SOMO in the $^2B_2$ state is the $6b_2$ orbital formed the antibonding combination of a small portion of the copper d_{xz} orbital and a large contribution of the in-plane O_2 π^* antibonding MO. In the $^2A_1$ state, the SOMO ($12a_1$) corresponds basically to a combination of the 4s and $4p_x$ copper MOs. Finally, in the $^2B_1$ state, the SOMO ($4b_1$) is an antibonding combination of the copper d_{xy} orbital with the out-of-plane O_2 π bonding MO.

The C_{2v} form of CuO_2 can be transformed into the C_s isomer by simply moving the O_2 moiety along the z-axis (see Figure 2). This movement connects the $^2A_2$ and $^2B_2$ states of the C_{2v} symmetry species with the ^2A" and ^2A' states in the C_s structure, respectively. In the $^2A''(C_s)$ state, the SOMO (6a") mainly corresponds to the antibonding combination of the d_{yz} and d_{x2-y2} orbitals for the copper with the $\pi*$ out-of-plane antibonding MO of O_2, the latter with a larger coefficient. In the $^2A'(C_s)$ state, the

SOMO (17a') is formed by the combination of the d_{xy} and d_{yz} orbitals of the copper with a small coefficient and a large contribution of the in-plane O_2 π^* antibonding MO. These 6a" and 17a' MOs are closely related to the C_{2v} $2a_2$ and $6b_2$ MOs, respectively. As we will see next, the energy differences between ^{2}A" and $^2A_2$ and also between ^{2}A' and $^2B_2$ are in general small for all methods of calculation analyzed. Indeed, an exceedingly flat PES is found in the direction that transforms the $^2A_2$ C_{2v} stationary point into the ^{2}A" C_s minimum.[37,40,41]

In all states (except for the $^2A_1$), the Cu–O_2 interaction is characterized by the drop of the unpaired 4s electron of Cu to the π^* antibonding MOs of O_2.[38,40] So, the bonding is essentially ionic (Cu^+–$O_2^{\cdot-}$) with some covalent contributions coming basically from the interactions between the O_2 π^* MOs and the Cu unoccupied 4p orbitals of suitable symmetry.[40] Interestingly, in the C_s structure the 4s Cu orbital can participate in the mixing and, therefore, the end-on structure has a somewhat large covalent character[38,40] as can be corroborated by the Mulliken charges on Cu atoms given in the Table S8 of the supporting information.

With respect to the geometrical parameters, Table 1 shows that the changes of the α_{CuOO} angle are especially important in the ^{2}A'' electronic state ranging from 108.9º at the CCSD(T) level to 120.4º with the HCTC functional, as a consequence of the PES being very flat around the ^{2}A'' minimum. The CCSD(T) optimized $R_{O\text{-}O}$ bond distance for ^{2}A" and $^2A_2$ is 1.330 and 1.374 Å, respectively. The larger value in the $^2A_2$ electronic state is a consequence of its higher ionicity which translates into larger O_2 π^* population. These O–O bond lengths in CuO_2 are much closer to that of $^2\Pi_g$ $O_2^{\cdot-}$ (exp.: 1.35 Å;[89] CCSD(T): 1.354 Å) than that of neutral $^3\Sigma_g^-$ O_2 (exp.: 1.208 Å;[89] CCSD(T): 1.211 Å) for most of the electronic states analyzed and theoretical methods used (see Table S10 in the supporting information) as expected from the essential ionic nature of the chemical bond in CuO_2. This is also reflected in the harmonic frequencies corresponding to the O–O stretching (see Tables S11-S17 of the supporting information). For the $^2A_1$ state, the O–O bond length is the shortest at the CCSD(T) level, which is not unexpected given the fact that the SOMO in this state ($12a_1$) does not have O–O π^* antibonding contribution. Conversely, for the $^2B_1$ state, the O–O bond length is the longest at all levels of theory ranging from 1.939 Å in CCSD(T) to 1.522 Å

in HF. The change from the $^2A_2$ to the $^2B_1$ electronic states involves the promotion of an electron from the $4b_1$ orbital, with an O–O π bonding contribution, to the $2a_2$ with an O–O π^* antibonding character. Consequently, there is an important increase in the R_{O-O} bond distance together with a reduction of the ν(O-O) harmonic frequency. In fact, in the $^2B_1$ stationary point, the O–O bond is broken and the CuO_2 complex has to be considered as an OCuO angular species. For all cases, except for the $^2A_2$ state at the HF level and the ^2A" state computed with the VSXC, HCTH, and TPSS functionals, the R_{Cu-O} distance is slightly larger for the related ^2A" and $^2A_2$ than for the ^2A' and $^2B_2$ states, respectively. As discussed by Bauschlicher et al.,[40] this has to be ascribed to the lower Cu–O_2 Pauli repulsion in the ^2A' and $^2B_2$ states as a result of having three electrons (as opposed to four in the ^2A" and $^2A_2$ states) occupying in-plane O_2 π^* orbitals. In spite of that, electrostatic interactions are more favorable when there are four electrons in the in-plane O_2 π^* orbitals which explains the higher stability of the ^2A" and $^2A_2$ states as compared to the ^2A' and $^2B_2$ states, respectively (*vide infra*). Let us notice that for all states except the $^2B_1$, there is a reduction of the Cu–O bond length when going from HF to CCSD(T) result. This behavior is opposed to the usual increase in the bond lengths when correlation effects are included and it is likely to be the result of important contributions of the excitations starting from the $6b_2$ and $2a_2$ orbitals, of similar energies and Cu–O antibonding character, to orbitals of higher energy with Cu–O nonbonding character.

In Table 2, we list the standard deviation (STD) of the geometrical parameters given in Table 1 as compared to the CCSD(T)/6-311+G(d) optimized parameters in each state. This number gives an idea of the performance of the different functionals for geometric parameters. It is worth noting the relatively good behavior of the HF method for geometries (with the exception of the $^2B_1$ state for which non-dynamical correlation could be important), which is not totally surprisingly given the well-known good performance of the HF method for ionic species. In spite of that, the HF results are outperformed by all DFT functionals except for the BHandH, M05, and HCTH which show a similar performance to that of the HF method.

It can be observed in Table 3 that, at the CCSD(T)/6-311+G(d) level, the ground electronic state of CuO_2 doublet is the $^2A_2$ (C_{2v}) and the relative stability of the different

electronic states is $^2A_2(C_{2v}) < {}^2A''(C_s) < {}^2B_2(C_{2v}) < {}^2A'(C_s) << {}^2A_1(C_{2v}) < {}^2B_1(C_{2v})$. The same relative stability order is obtained with single point energies calculations at the optimized CCSD(T)/6-311+G(d) geometries using the aug-cc-pVTZ and aug-cc-pVQZ basis sets and extrapolating to the CBS limit. However, at the CBS limit (Table 4), the difference between $^2A_2$ and $^2A''$ increases from 0.03 kcal mol^{-1} to 1.4 kcal mol^{-1}. In Table 5 we provide the geometries and energy differences found with the CCSD(T) method using the aug-cc-pVTZ and aug-cc-pVQZ basis sets. As can be seen, in comparison with the 6-311+G(d) results, the Cu–O bond contracts by 0.02 – 0.03 Å with these basis sets, but energy differences remain unchanged. Our best estimate for the energy difference between the $^2A_2$ and the $^2A''$ lowest-energy states is 1.38 kcal mol^{-1}, the $^2A_2$ being the most stable. It is important to remark that this energy difference is converged with respect to the basis set (see Tables 4 and 5) and optimized geometry (compare the results with the CCSD(T)/6-311+G(d) and CCSD(T)/aug-cc-pVQZ geometries). The higher stability of the side-on $^2A_2$ as compared to end-on $^2A''$ species in the gas-phase was already found previously at the CASPT2[37] and CCSD(T)[40,41] correlated levels, the energy difference reported being similar to that found in the present study (CASPT2 = 0.5[37] kcal mol^{-1}; CCSD(T) = 0.74[40,41] and 0.9[40,41] kcal mol^{-1}). As said in the Introduction, EPR experiments[29-31] show two magnetically inequivalent oxygen atoms and this had been taken as an indication that the end-on C_s structure is the ground state. CASPT2 calculations by Roos et al.[37] indicate that the gas-phase ground state is the side-on $^2A_2$ state but because of the small energy difference between the two species, the $^2A''$ C_s structure, which has a large dipole moment, becomes the ground-state in rare-gas matrices.

The relative stability of the different electronic states found by the HF and DFT analyzed methods is $^2A''(C_s) < {}^2A_2\,(C_{2v}) < {}^2A'(C_s) < {}^2B_2\,(C_{2v}) << {}^2A_1\,(C_{2v}) < {}^2B_1\,(C_{2v})$. Unfortunately, for the BLYP, G96LYP, and mPWPW91 methods, we were unable to converge the $^2B_1$ state. As found in previous studies,[19,20,37,38] our HF and DFT results indicates that the end-on C_s structure is more stable than the side-on C_{2v} species by about 10 kcal mol^{-1}. Only the HF and BHandH yield side-on $^2A_2(C_{2v})$ and end-on $^2A''(C_s)$ species of comparable energy (about 2 kcal mol^{-1} difference). When all electronic states are considered, the standard deviation values (last row of Table 3) indicate that B3LYP and B3LYP* are the methods that globally give the more similar results to the data obtained using CCSD(T)/6-311+G(d). All STD given by the DFT

methods are smaller than the HF STD except for the M05, VSXC, HCTH, and TPSS functionals. If we take the STD for all states except the $^2B_1$, then only the mPWPW91, B3LYP, B3LYP*, and BHandH perform better than HF.

The side-on $^2A_2(C_{2v})$ and end-on $^2A''(C_s)$ species are almost isoenergetic according to our HF, BHandH, and CCSD(T) results. The fact that most DFT methods such as the B3LYP clearly favor by about 10 kcal mol^{-1} the end-on $^2A''$ state as compared to $^2A_2$ one is due, in part, to the fact that the $^2A_2$ state has a larger ionic character (*vide supra*) than the $^2A''$ state. Therefore, its stability is underestimated by most DFT methods because these methods overestimate the Cu first IP (see Table S18, exp.: 7.72 eV;[90] CCSD(T)/CBS limit: 7.54 eV; CCSD(T)/6-311+G(d): 7.26 eV; B3LYP/6-311+G(d): 8.04 eV). Since the CCSD(T) method yields a low IP as compared to the experimental value, the possibility of the $^2A_2$ state being overstabilized by CCSD(T) methods cannot be rule out.[38]

Let us finish this section by analyzing the binding energies (BEs) of CuO_2 ground state with respect to the Cu (^2S) and O_2 ($^3\Sigma_g^-$) fragments for the different levels of calculation listed in Table 6. The considered CuO_2 ground state is ^2A" for HF and DFT methods and $^2A_2$ for the CCSD(T) method. This BE was measured experimentally by Mitchell to be 15±5 kcal mol^{-1}.[36] The CCSD(T) result we have obtained with the aug-cc-pVTZ and aug-cc-pVQZ basis sets at their respective optimized geometries is 13.78 and 13.81 kcal mol^{-1} in good agreement with the experimental value. Surprisingly, the BE obtained at the CCSD(T)/6-311+G(d) level is clearly two low by about 10 kcal mol^{-1} in comparison to the experiment and the CCSD(T) result obtained at the CBS limit, which points out the importance of the basis set at this level of theory for obtaining an accurate binding energy. For the present system, and due to the nature of the bonding (Cu^+-$O_2^{\cdot -}$), it is particularly important to accurately describe the electron affinity (EA) of O_2, which at the CCSD(T) level requires large basis sets with multiple diffuse and polarization functions. Note that the CCSD(T) EA of O_2 is computed to be 0.03, 0.36 and 0.38 eV with the 6-311+G(d), aug-ccpVDZ and aug-ccpVTZ basis sets, respectively, the experimental value being 0.448±0.006 eV.[91] Most functionals with the exception of VSXC give binding energies ranging from 10 to 20 kcal mol^{-1} and therefore within the experimental result. On the contrary, the HF value of −11.1 kcal

mol^{-1} indicates that this method erroneously considers CuO_2 as a metastable species. As compared to the experimental value, the B3LYP* functional yields the closest result.

Table 6, here

B. On the Optimal Mixing of HF exchange in B3LYP-like Functionals for the CuO_2 description

It is well-known that estimations of IPs are usually better when using hybrid methods with a large percentage (about 40%) of HF exchange.[54,92] To explore whether hybrid methods with increasing degree of HF exchange can reproduce better the CCSD(T) results, we have calculated the different electronic states of CuO_2 doublet by varying monotonically the proportion of exact exchange introduced in B3LYP-like functionals. We have made use of the Gaussian 03 program feature that allows one to vary the B3LYP standard Becke parameter set (PS) through internal options.

We have changed the a_o parameter by 0.100 increments in the interval $0.100 \leq a_o \leq 0.900$, with fixed $a_x = 1 - a_o$ and $a_c = a_x$. The $a_x = 1 - a_o$ relationship has already been used in some hybrid functionals.[79,93] We also found in previous works[48] that the $a_x = 1 - a_o$ and $a_c = a_x$ relations between the B3LYP parameters are, on average, the optimal ones to minimize the difference between the actual B3LYP density and the QCISD one in a series of small molecules. For this reason the relationships between a_x and a_o and a_c mentioned previously will be maintained throughout this work. However, neither the choice that we have employed here nor other possible alternative relations among the three parameters should be considered as universal.[48,79] In Table S1, we list the different PSs $\{a_o,a_x,a_c\}$ employed.

The optimized geometric parameters and the STD of the optimized geometrical parameters as a function of a_o are collected in Tables 7 and 8, while Table 9 contains the relative energies of different electronic states obtained with the different PSs. The HF values have been included for comparison purposes. For the C_{2v} $^2A_2$ and $^2B_2$ states (and also for the related C_s ^2A" and ^2A'), the $R_{O\text{-}O}$ bond distance decreases with the increase of the a_o parameter. In general, this is the expected behavior when increasing the portion of HF exchange[46] in the functional since HF distances are usually shorter than

correlated ones. This reduction in the R_{O-O} bond distance goes with a steady increase in the α_{CuOO} angle when going from BLYP to HF. Finally, the Cu–O bond increases with the growth in the a_o parameter, especially in the $^2B_2$ state. This is the result of the Cu–O bond distance being longer at the HF level, for the reasons discussed before. In addition, the Cu–O bond becomes more ionic when a_o increases. The energy of the 4s Cu orbital keeps approximately constant while the O_2 π^* orbitals are stabilized, so both orbitals become more distant in energy when a_o increases and this favors the charge transfer from Cu to O_2 for the C_{2v} $^2A_2$ and $^2B_2$ states. This is confirmed by the Mulliken charges of Table S8 in the supporting information. The $^2A_1$ and $^2B_1$ states remain essentially unmodified by variations of the a_o parameter, except for the R_{O-O} bond distance in the $^2B_1$ state that increases for smaller a_o values. The increase in the a_o parameter leads to a stabilization of the 3d Cu and O_2 π orbitals. Since the stabilization is smaller for the 3d orbitals, one gets smaller amplitudes of the O_2 π orbitals (and higher for the intervening 3d orbitals) in the $4b_1$ orbital which is singly occupied in the $^2B_1$ state. As a consequence, the R_{O-O} bond distance in this state is larger for smaller a_o values.

Tables 7-9, here

In Table 8, we gather the STD of the geometrical parameters given in Table 6. The smaller STD values are attained for PS = 2 to 5 ($0.2 < a_o < 0.5$), which is consistent with the fact that for the DFT methods tested previously the smaller STD values were obtained for B3LYP ($a_o = 0.2$) and for B3LYP* ($a_o = 0.15$).

The relative stability of the different electronic states found by different B3LYP-like functionals analyzed methods is the same as that found for the rest of DFT methods, i.e., $^2A''(C_s) < {}^2A_2(C_{2v}) < {}^2A'(C_s) < {}^2B_2(C_{2v}) << {}^2A_1(C_{2v}) < {}^2B_1(C_{2v})$ (see Table 9). Although in all cases the ground state of CuO_2 is the $^2A''$, when we increase the a_o parameter the difference in energy between the $^2A''$ and $^2A_2$ decreases. For the PS9, the values for the relative energies for the $^2A''$ and $^2A_2$ electronic states are quite close to the ones obtained with CCSD(T). We attributed this behavior to the larger ionic character of the $^2A_2$ state. Ionic states are overstabilized by the HF method. Therefore, a functional containing large proportion of HF exchange stabilizes the $^2A_2$ state as compared to the $^2A''$ state. Indeed, the HF method outperforms most of DFT functionals as far as the energy differences between $^2A''$ and $^2A_2$ is concerned. The

increase in the a_o parameter leads also to smaller energy differences between the $^2A_2$ and $^2B_2$ states. The reason can be found in the stabilization of the 3d Cu and O_2 π^* orbitals for large a_o values. The stabilization is slightly larger for the 3d orbitals and this leads to larger amplitudes of the O_2 π^* orbitals (and smaller for the intervening 3d orbitals) in the $6b_2$ and $2a_2$ orbitals which are singly or doubly occupied in the $^2A_2$ and $^2B_2$ states. Thus, for larger a_o values one has longer Cu–O bonds (*vide supra*) and more similar $6b_2$ and $2a_2$ orbitals, which become almost pure O_2 π^* orbitals. This leads to smaller energy differences between the $^2A_2$ and $^2B_2$ states (and the same for the ^2A" and ^2A' states). The trends for the $^2A_1$ and $^2B_1$ states are less clear. In general, PS1, PS2 and PS3 ($0.1 < a_o < 0.3$) are the parameter sets that globally give the most similar energies for the studied electronic states to the data obtained with the CCSD(T) method using the same 6-311+G(d) basis set. As it has been mentioned before, B3LYP (a_o = 0.2) and B3LYP* (a_o = 0.15) give, globally and among the DFT methods studied, the more similar results to the data obtained using CCSD(T). Somewhat unexpectedly, for relative energies the B3LYP-like functional with a larger contribution of exact exchange (90%) is the one giving the smaller standard deviation when the $^2B_1$ state is not included in the calculation. Binding energies obtained with the different PSs are collected in Table S19.

It is known that in odd electron systems the self-interaction error (SIE) can be potentially important and artificially stabilize delocalized states. Hybrid functionals show smaller SIEs than pure functionals because they include a HF exchange portion. Therefore, one could hypothesize that the stabilization of the $^2A_2$ as compared to ^2A" when increasing the a_o value (and also of the $^2B_2$ with respect to the $^2A_2$) is due to the effect of SIE. In Figure 3, the spin density on the Cu atom is depicted as a function of the a_o parameter for the C_{2v} electronic states respectively. As can be seen, we have three different situations. For the $^2A_2$ and $^2B_2$ electronic states (and the same occurs in the ^2A" and ^2A' states), the increase of the a_o parameter causes no change in the localization of the unpaired electron, since it remains completely localized on the O_2 moiety. So, this result indicates that the SIE should be similar for these states and should have no influence in the change of relative energies. On the other hand, for the $^2A_1$ electronic state, for low a_o values the spin is on the copper, which means that basically we have Cu interacting with O_2. With the increase in the a_0 parameter, the $^2A_1$ electronic state

evolves to Cu^+ and $O_2^{\cdot -}$. Finally, for the $^2B_1$ electronic state, the spin density on Cu^+ increases from approximately 0.2 to 0.9 with the increase in the a_o parameter, which is a consequence of the decrease of O participation in the $4b_1$ for larger a_o values.

Figure 3, here

In Table 10 we list the number of imaginary frequencies found for the located C_{2v} and C_s stationary points with the different methods used and for the set of electronic states analyzed. CCSD(T) frequencies have been computed by a numerical procedure. Since the asymmetric stretching mode breaks the C_{2v} symmetry, the numerical calculation of the frequencies is only possible for the two lowest-lying $^2A_2$ and $^2B_2$ states, which are related with the ^2A" and ^2A' states in C_s symmetry. It is interesting to verify that the nature of the functional and the percentage of HF exchange in B3LYP-like functionals modify the nature of the stationary points. Indeed, the HF, BLYP, G96LYP, OLYP, OPBE, mPWPW91, B3LYP, B3LYP*, M05, HCTH, TPSS, and B3LYP-like functionals with PS = 0 to 5 predict an imaginary frequency for the $^2A_2$ electronic state. So, this C_{2v} stationary point is found to be a transition state connecting two ^2A" equivalent minima. Only, the HandH, VSXC, and B3LYP-like functionals with PS = 6 to 9 point out, like the CCSD(T) method, that this species is a minimum. On the other hand, HF and B3LYP-like functionals with PS = 4 to 9 indicates that the $^2B_2$ C_{2v} species is a transition state connecting two ^2A" equivalent minima. Indeed, only the BHandH and the VSXC functionals correctly predicts the correct number (zero) of imaginary frequencies for the ^2A", ^2A', $^2A_2$, and $^2B_2$ electronic states.

Table 10, here

CONCLUSIONS

The ground and low-lying states of doublet CuO_2 have been studied using different density functional and CCSD(T) methods. At the CCSD(T) level, the CuO_2 doublet presents C_{2v} geometry and the ground electronic state is a $^2A_2$ state. The end-on C_s ^2A'' electronic state lies, however, less than 1 kcal mol^{-1} above. Moreover, at the CCSD(T) level of theory the relative order of the electronic states is $^2A_2(C_{2v}) < {}^2A''(C_s) < {}^2B_2(C_{2v}) < {}^2A'(C_s) << {}^2A_1(C_{2v}) < {}^2B_1(C_{2v})$. These results are reproduced by none of

the DFT functionals that have been used, since in all cases the computed ground state is the $^2A''$ with an end-on C_s geometry. The reason for the DFT computed higher stability of the $^2A''$ relative to $^2A_2$ state can not be attributed to a higher electron delocalization in the $^2A''$ state and must be ascribed to its larger covalent character. The relative energy between the $C_{2v}(^2A_2)$ and $C_s(^2A'')$ structures computed for the different functionals ranges between 2 and 16 kcal mol^{-1}, the functional that better compares with CCSD(T) being the BHandH one. However, when one compares the best geometries and relative energies with respect to CCSD(T) results for *all* the different electronic states analyzed, it is found that B3LYP gives the smallest standard deviations. As to the effect of the a_o parameter is concerned, it is found that the B3LYP-like functional yielding better geometries contains 20% of exact exchange, although somewhat unexpectedly, for relative energies the B3LYP-like functional with a larger contribution of exact exchange (90%) is the one giving the smaller standard deviation. Interestingly, only the BHandH and the VSXC functionals correctly predicts the correct number (zero) of imaginary frequencies for the $^2A''$, $^2A'$, $^2A_2$, and $^2B_2$ electronic states.

From our calculations it is clear that only high level *ab initio* methods providing a good estimation of correlation energy (such as MCSCF or CCSD) are able to give the correct relative energies of the different states in CuO_2. Since such methods are usually not affordable for large $L_nCu^I\text{-}O_2^{-\cdot}$ species, the functional of choice for these cases should be the B3LYP method for geometry optimizations followed by single point calculations with a B3LYP-like functional containing a large percentage of HF exchange (for instance, PS 9).

Acknowledgments

This study was financially supported by the Spanish research projects no. CTQ2005-08797-C02-01/BQU and CTQ2008-03077/BQU and the DURSI project nr. 2005SGR-00238. M.G. thanks the Spanish MEC for Ph.D. grant.

Supporting Information Available. Figure S1 with a schematic representation of interaction between the Cu (^2S) and O_2 ($^3\Sigma_g^-$) fragments in the $^2B_2$ electronic state of the C_{2v} CuO_2 species.

Tables S1-S19 with the parameter sets analyzed, the S^2 values, pictures of molecular orbitals for all electronic states, Mulliken charges, O–O bond distances in O_2 and O_2^-, calculated harmonic vibrational frequencies, ionization potentials, and binding energies for all electronic states analyzed.

REFERENCES

(1) Rosenzweig, A. C.; Sazinsky, M. H. *Curr. Op. Struct. Biol.* **2006**, *16*, 729.
(2) MacPherson, I. S.; Murphy, M. E. P. *Cell. Mol. Life Sci.* **2007**, *64*, 2887.
(3) Punniyamurthy, T.; Velusamy, S.; Iqbal, J. *Chem. Rev.* **2005**, *105*, 2329.
(4) Holm, R. H.; Kennepohl, P.; Solomon, E. I. *Chem. Rev.* **1996**, *96*, 2239.
(5) Bento, I.; Carrondo, M. A.; Lindley, P. F. *J. Biol. Inorg. Chem.* **2006**, *11*, 539.
(6) Miller, A. F. *Curr. Op. Chem. Biol.* **2004**, *8*, 162.
(7) Fridovich, I. *J. Biol. Chem.* **1997**, *272*, 18515.
(8) Hart, P. J.; Balbirnie, M. M.; Ogihara, N. L.; Nersissian, A. M.; Weiss, M. S.; Valentine, J. S.; Eisenberg, D. *Biochemistry* **1999**, *38*, 2167.
(9) Torrent, M.; Solà, M.; Frenking, G. *Chem. Rev.* **2000**, *100*, 439.
(10) Himo, F.; Siegbahn, P. E. M. *Chem. Rev.* **2003**, *103*, 2421.
(11) Siegbahn, P. E. M.; Blomberg, M. R. A. *Chem. Rev.* **2000**, *100*, 421.
(12) Siegbahn, P. E. M.; Blomberg, M. R. A. *Ann. Rev. Phys. Chem.* **1999**, *50*, 221.
(13) Poater, J.; Solà, M.; Rimola, A.; Rodríguez-Santiago, L.; Sodupe, M. *J. Phys. Chem. A* **2004**, *108*, 6072.
(14) Braida, B.; Hiberty, P. C.; Savin, A. *J. Phys. Chem. A* **1998**, *102*, 7872.
(15) Sodupe, M.; Bertran, J.; Rodríguez-Santiago, L.; Baerends, E. J. *J. Phys. Chem. A* **1999**, *103*, 166.
(16) Chermette, H.; Ciofini, I.; Mariotti, F.; Daul, C. *J. Chem. Phys.* **2001**, *115*, 11068.
(17) Bartlett, R. J. *Ann. Rev. Phys. Chem.* **1981**, *32*, 359.
(18) Raghavachari, K.; Trucks, G. W.; Pople, J. A.; Headgordon, M. *Chem. Phys. Lett.* **1989**, *157*, 479.
(19) Pouillon, Y.; Massobrio, C. *Chem. Phys. Lett.* **2000**, *331*, 290.
(20) Chertihin, G. V.; Andrews, L.; Bauschlicher Jr., C. W. *J. Phys. Chem. A* **1997**, *101*, 4026.
(21) Zhao, Y.; Truhlar, D. G. *Acc. Chem. Res.* **2008**, *41*, 157.
(22) Schultz, N. E.; Zhao, Y.; Truhlar, D. G. *J. Phys. Chem. A* **2005**, *109*, 11127.
(23) Schultz, N. E.; Zhao, Y.; Truhlar, D. G. *J. Phys. Chem. A* **2005**, *109*, 4388.
(24) Neese, F. *J. Biol. Inorg. Chem.* **2006**, *11*, 702.
(25) Quintal, M. M.; Karton, A.; Iron, M. A.; Boese, A. D.; Martin, J. M. L. *J. Phys. Chem. A* **2006**, *110*, 709.
(26) Zhao, Y.; Truhlar, D. G. *J. Chem. Phys.* **2006**, *124*, 224105.
(27) Zhao, Y.; Truhlar, D. G. *Theor. Chem. Acc.* **2008**, *120*, 215.
(28) Tevault, D. E. *J. Chem. Phys.* **1982**, *76*, 2859.
(29) Howard, J. A.; Sutcliffe, R.; Mile, B. *J. Phys. Chem.* **1984**, *88*, 4351.
(30) Kasai, P. H.; Jones, P. M. *J. Phys. Chem.* **1986**, *90*, 4239.
(31) Mattar, S. M.; Ozin, G. A. *J. Phys. Chem.* **1988**, *92*, 3511.
(32) Ozin, G. A.; Mitchell, S. A.; Garcia-Prieto, J. *J. Am. Chem. Soc.* **1983**, *105*, 6399.
(33) Wu, H.; Desai, S. R.; Wang, L.-S. *J. Phys. Chem. A* **1997**, *101*, 2103.
(34) Bondybey, V. E.; English, J. H. *J. Phys. Chem.* **1984**, *88*, 2247.
(35) Uzunova, E. L.; Mikosch, H.; Nikolov, G. S. *J. Chem. Phys.* **2008**, *128*, 094307.
(36) Mitchell, S. A. *Gas Phase Metal Reactions*, Fontijn, A. ed.; Elsevier: Amsterdam, 1992.
(37) Hasegawa, J.; Pierloot, K.; Roos, B. O. *Chem. Phys. Lett.* **2001**, *335*, 503.
(38) Barone, V.; Adamo, C. *J. Phys. Chem.* **1996**, *100*, 2094.
(39) Mochizuki, Y.; Nagashima, U.; Yamamoto, S.; Kashiwagi, H. *Chem. Phys. Lett.* **1989**, *164*, 225.
(40) Bauschlicher Jr., C. W.; Langhoff, S. R.; Partridge, H.; Sodupe, M. *J. Phys. Chem.* **1993**, *97*, 856.
(41) Hrusák, J.; Koch, W.; Schwarz, H. *J. Chem. Phys.* **1994**, *101*, 3898.
(42) Poater, J.; Solà, M.; Duran, M.; Robles, J. *Phys. Chem. Chem. Phys.* **2002**, *4*, 722.
(43) Latajka, Z.; Bouteiller, Y.; Scheiner, S. *Chem. Phys. Lett.* **1995**, *234*, 159.

(44) Lundell, J.; Latajka, Z. *J. Phys. Chem. A* **1997**, *101*, 5004.
(45) Hoe, W. M.; Cohen, A. J.; Handy, N. C. *Chem. Phys. Lett.* **2001**, *341*, 319.
(46) Csonka, G. I.; Nguyen, N. A.; Kolossváry, I. *J. Comput. Chem.* **1997**, *18*, 1534.
(47) Chermette, H.; Razafinjanahary, H.; Carrion, L. *J. Chem. Phys.* **1997**, *107*, 10643.
(48) Poater, J.; Duran, M.; Solà, M. *J. Comput. Chem.* **2001**, *22*, 1666.
(49) Durant, J. L. *Chem. Phys. Lett.* **1996**, *256*, 595.
(50) Lynch, B. J.; Truhlar, D. G. *J. Phys. Chem. A* **2001**, *105*, 2936.
(51) Lynch, B. J.; Fast, P. L.; Harris, M.; Truhlar, D. G. *J. Phys. Chem. A* **2000**, *104*, 4811.
(52) Kormos, B. L.; Cramer, C. J. *J. Phys. Org. Chem.* **2002**, *15*, 712.
(53) Kalaiselvan, A.; Venuvanalingam, P.; Poater, J.; Solà, M. *Int. J. Quantum Chem.* **2005**, *102*, 139.
(54) Abu-Awwad, F.; Politzer, P. *J. Comput. Chem.* **2000**, *21*, 227.
(55) Dkhissi, A.; Alikhani, M. E.; Bouteiller, Y. *J. Mol. Struct. (Theochem)* **1997**, *416*, 1.
(56) Wilson, P. J.; Tozer, D. J. *J. Chem. Phys.* **2002**, *116*, 10139.
(57) Reiher, M.; Salomon, O.; Hess, B. A. *Theor. Chem. Acc.* **2001**, *107*, 48.
(58) Becke, A. D. *J. Chem. Phys.* **1993**, *98*, 5648.
(59) Reiher, M. *Inorg. Chem.* **2002**, *41*, 6928.
(60) Swart, M.; Groenhof, A. R.; Ehlers, A. W.; Lammertsma, K. *J. Phys. Chem. A* **2004**, *108*, 5479.
(61) Handy, N. C.; Cohen, A. J. *Mol. Phys.* **2001**, *102*, 403.
(62) Perdew, J. P.; Burke, K.; Ernzerhof, M. *Phys. Rev. Lett.* **1996**, *77*, 3865.
(63) Güell, M.; Luis, J. M.; Solà, M.; Swart, M. *J. Phys. Chem. A* **2008**, *112*, 6384.
(64) Frisch, M. J.; Trucks, G. W.; Schlegel, H. B.; Scuseria, G. E.; Robb, M. A.; Cheeseman, J. R.; Montgomery Jr., J. A.; Vreven, T.; Kudin, K. N.; Burant, J. C.; Millam, J. M.; Iyengar, S. S.; Tomasi, J.; Barone, V.; Mennucci, B.; Cossi, M.; Scalmani, G.; Rega, N.; Petersson, G. A.; Nakatsuji, H.; Hada, M.; Ehara, M.; Toyota, K.; Fukuda, R.; Hasegawa, J.; Ishida, M.; Nakajima, T.; Honda, Y.; Kitao, O.; Nakai, H.; Klene, M.; Li, X.; Knox, J. E.; Hratchian, H. P.; Cross, J. B.; Bakken, V.; Adamo, C.; Jaramillo, J.; Gomperts, R.; Stratmann, R. E.; Yazyev, O.; Austin, A. J.; Cammi, R.; Pomelli, C.; Ochterski, J. W.; Ayala, P. Y.; Morokuma, K.; Voth, G. A.; Salvador, P.; Dannenberg, J. J.; Zakrzewski, G.; Dapprich, S.; Daniels, A. D.; Strain, M. C.; Farkas, O.; Malick, D. K.; Rabuck, A. D.; Raghavachari, K.; Foresman, J. B.; Ortiz, J. V.; Cui, Q.; Baboul, A. G.; Clifford, S.; Cioslowski, J.; Stefanov, B. B.; Liu, G.; Liashenko, A.; Piskorz, P.; Komaromi, I.; Martin, R. L.; Fox, D. J.; Keith, T.; Al-Laham, M. A.; Peng, C. Y.; Nanayakkara, A.; Challacombe, M.; Gill, P. M. W.; Johnson, B.; Chen, W.; Wong, M. W.; Gonzalez, C.; Pople, J. A. Gaussian 03; Gaussian 03, Revision C.01 ed.; Gaussian, Inc.: Pittsburgh, PA, 2003.
(65) Werner, H.-J.; Knowles, P. J.; Lindh, R.; Manby, F. R.; Schütz, M.; etal. MOLPRO, version 2006.1, a package of ab initio programs, 2006.
(66) Wachters, A. J. H. *J. Chem. Phys.* **1970**, *52*, 1033.
(67) In the Gaussian 03 implementation of the Cu basis set, the s and p functions come from Wachter's optimization for the Cu atom in its ^{2}S state, while the d functions come from Wachter's optimization for the Cu atom in its ^{2}D state. In addition, we have checked that with the B3LYP method the Gaussian 03 internal basis set provides much reasonable results for the relative energies among the different analyzed states than the basis set with the d functions coming from Wachter's optimization for the Cu atom in its ^{2}D state.
(68) Dunning Jr., T. H. *J. Chem. Phys.* **1989**, *90*, 1007.
(69) Halkier, A.; Helgaker, T.; Jørgensen, P.; Klopper, W.; Koch, H.; Olsen, J.; Wilson, A. K. *Chem. Phys. Lett.* **1998**, *286*, 243.
(70) Lee, C. T.; Yang, W. T.; Parr, R. G. *Phys. Rev. B* **1988**, *37*, 785.
(71) Becke, A. D. *Phys. Rev. A* **1988**, *38*, 3098.
(72) Perdew, J. P.; Chevary, J. A.; Vosko, S. H.; Jackson, K. A.; Pederson, M. R.; Singh, D. J.; Fiolhais, C. *Phys. Rev. B* **1992**, *46*, 6671.
(73) Perdew, J. P.; Chevary, J. A.; Vosko, S. H.; Jackson, K. A.; Pederson, M. R.; Singh, D. J.; Fiolhais, C. *Phys. Rev. B* **1993**, *48*, 4978.
(74) Perdew, J. P.; Burke, K.; Wang, Y. *Phys. Rev. B* **1998**, *57*, 14999.

(75) Perdew, J. P.; Burke, K.; Wang, Y. *Phys. Rev. B* **1996**, *54*, 16533.
(76) Stephens, P. J.; Devlin, F. J.; Chabalowski, C. F.; Frisch, M. J. *J. Phys. Chem.* **1994**, *98*, 11623.
(77) Vosko, S. H.; Wilk, L.; Nusair, M. *Can. J. Phys.* **1980**, *58*, 1200.
(78) Hertwig, R. H.; Koch, W. *Chem. Phys. Lett.* **1997**, *268*, 345.
(79) Burke, K.; Ernzerhof, M.; Perdew, J. P. *Chem. Phys. Lett.* **1997**, *265*, 115.
(80) Gill, P. M. W. *Mol. Phys.* **1996**, *89*, 433.
(81) Perdew, J. P.; Wang, Y. *Phys. Rev. B* **1992**, *45*, 13244.
(82) Becke, A. D. *J. Chem. Phys.* **1993**, *98*, 1372.
(83) Zhao, Y.; Schultz, N. E.; Truhlar, D. G. *J. Chem. Phys.* **2005**, *126*, 161103.
(84) Van Voorhis, T.; Scuseria, G. E. *J. Chem. Phys.* **1998**, *109*, 400.
(85) Hamprecht, F. A.; Cohen, A. J.; Tozer, D. J.; Handy, N. C. *J. Chem. Phys.* **1998**, *109*, 6264.
(86) Tao, J. M.; Perdew, J. P.; Staroverov, V. N.; Scuseria, G. E. *Phys. Rev. Lett.* **2003**, *91*, 146401.
(87) Zhao, Y.; Schultz, N. E.; Truhlar, D. G. *J. Chem. Theory Comput.* **2006**, *2*, 364.
(88) Lee, T. J.; Rice, J. E.; Scuseria, G. E.; Schaefer III, H. F. *Theor. Chim. Acta* **1989**, *75*, 81.
(89) Huber, K. P.; Herzberg, G. *Molecular spectra and molecular structure*; Van Nostrand Reinhold: New York, 1979; Vol. 4.
(90) Lide, D. R., (Ed.) *CRC Handbook of Chemistry and Physics*; CRC Press: Boca Raton, 1998; Vol. 79th.
(91) Ervin, K. M.; Anusiewicz, I.; Skurski, P.; Simons, J.; Lineberger, W. C. *J. Phys. Chem. A* **2003**, *107*, 8521
(92) Salzner, U.; Lagowski, J. B.; Pickup, P. G.; Poirier, R. A. *J. Comput. Chem.* **1997**, *18*, 1943.
(93) Becke, A. D. *J. Chem. Phys.* **1996**, *104*, 1040.

FIGURE 1. Mechanism for the disproportionation of superoxide to give dioxygen and hydrogen peroxide in superoxide dismutase.

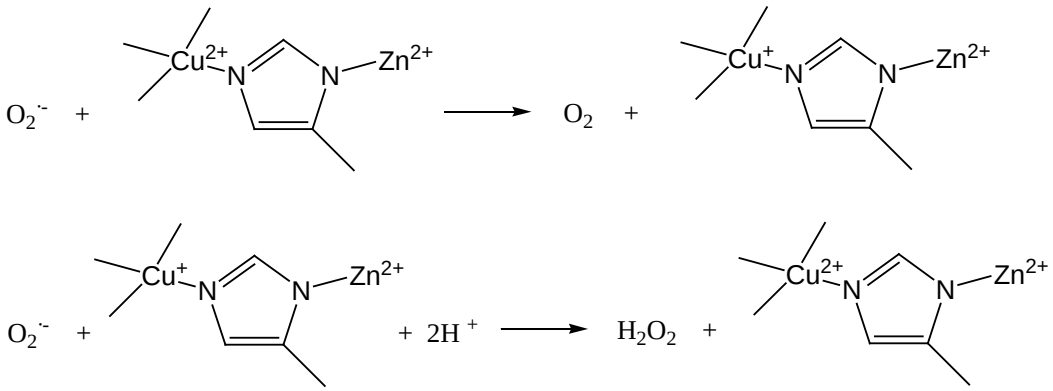

FIGURE 2. (a) Side-on (C_{2v}) and (b) end-on (C_s) structures of CuO_2.

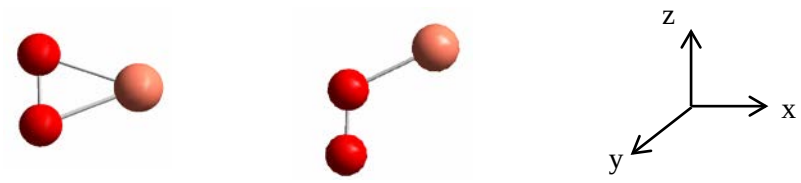

(a) **(b)**

FIGURE 3. Spin density (au) at the Cu atom for the C_{2v} CuO_2 species in different electronic states computed with the B3LYP method using different parameter sets (see Table S2).

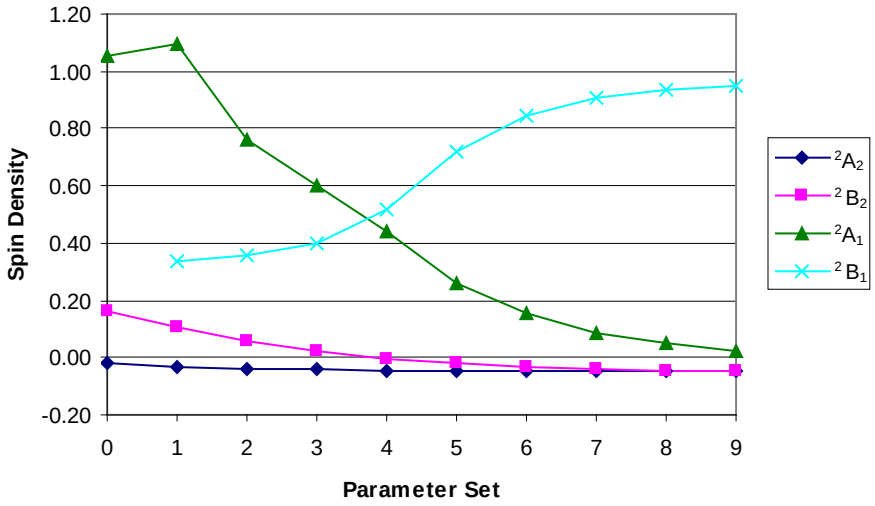

TABLE 1. Optimized Geometric Parameters[a] of the Ground and Low-Lying Electronic States of CuO_2 at Different Levels of Theory obtained with the 6-311+G(d) basis set.

symmetry	state	geometry	HF	BLYP	G96LYP	OLYP	OPBE	mPWPW91	B3LYP	B3LYP*	BHandH	M05	VSXC	HCTH	TPSS	CCSD(T)
C_s	$^2A''$	$R_{Cu\text{-}O}$[b]	1.915	1.907	1.906	1.974	1.940	1.893	1.911	1.904	1.839	1.907	1.922	1.946	1.876	1.878
		$R_{O\text{-}O}$	1.299	1.303	1.299	1.276	1.262	1.288	1.283	1.285	1.271	1.271	1.285	1.262	1.298	1.330
		α_{CuOO}	110.0	119.6	119.6	120.2	120.3	119.6	117.9	118.4	114.2	117.1	117.2	120.4	118.6	108.9
	$^2A'$	$R_{Cu\text{-}O}$[b]	1.900	1.825	1.820	1.838	1.824	1.810	1.826	1.821	1.798	1.839	2.051	2.105	1.967	1.849
		$R_{O\text{-}O}$	1.313	1.358	1.353	1.328	1.312	1.341	1.341	1.342	1.301	1.312	1.247	1.228	1.260	1.370
		α_{CuOO}	113.4	115.5	115.6	118.1	118.3	115.6	114.0	114.4	114.2	116.0	118.4	124.4	125.2	100.3
C_{2v}	$^2A_2$	$R_{Cu\text{-}O}$	2.070	2.007	2.000	2.018	2.003	1.990	2.009	2.004	1.968	2.024	2.011	2.014	1.983	2.014
		$R_{O\text{-}O}$	1.294	1.412	1.406	1.377	1.359	1.392	1.364	1.371	1.307	1.331	1.386	1.362	1.397	1.374
		α_{CuOO}	71.8	69.4	69.4	70.0	70.2	69.5	70.2	70.0	70.6	70.8	69.8	70.2	69.4	70.1
	$^2B_2$	$R_{Cu\text{-}O}$	2.091	1.925	1.918	1.934	1.915	1.907	1.952	1.937	1.841	1.974	1.935	1.934	1.900	1.981
		$R_{O\text{-}O}$	1.308	1.469	1.462	1.425	1.404	1.447	1.401	1.413	1.330	1.358	1.435	1.408	1.455	1.398
		α_{CuOO}	71.8	67.6	67.6	68.4	68.5	67.7	69.0	68.6	70.0	69.9	68.2	68.7	67.5	69.3
	$^2A_1$	$R_{Cu\text{-}O}$	2.036	2.039	2.026	2.063	2.010	1.998	2.022	2.016	1.938	2.220	2.047	2.117	1.967	1.931
		$R_{O\text{-}O}$	1.304	1.316	1.313	1.285	1.277	1.305	1.275	1.284	1.225	1.230	1.288	1.263	1.314	1.315
		α_{CuOO}	71.3	71.2	71.1	71.8	71.5	70.9	71.6	71.4	71.6	73.9	71.7	72.7	70.5	70.1
	$^2B_1$	$R_{Cu\text{-}O}$	1.830	–[c]	–[c]	1.893	1.878	–[c]	1.875	1.877	1.795	1.879	1.888	1.892	1.860	1.912
		$R_{O\text{-}O}$	1.522	–[c]	–[c]	1.777	1.735	–[c]	1.711	1.727	1.566	1.653	1.812	1.770	1.805	1.939
		α_{CuOO}	65.4	–[c]	–[c]	62.0	62.5	–[c]	62.9	62.6	64.1	63.9	61.3	62.1	61.0	61.0

[a] Distances are in angstroms and angles in degrees.
[b] Cu–O bond length corresponding to the shortest Cu–O distance.
[c] The SCF process in this state could not be converged.

TABLE 2. Standard Deviation Values (STD) for the Geometric Parameters[a] of CuO_2 in Different Electronic States with the 6-311+G(d) basis set.

symmetry	state	HF	BLYP	G96LYP	OLYP	OPBE	mPWPW91	B3LYP	B3LYP*	BHandH	M05	VSXC	HCTH	TPSS
C_s	$^2A''$	0.030	0.110	0.111	0.131	0.127	0.111	0.097	0.101	0.067	0.091	0.092	0.129	0.100
	$^2A'$	0.139	0.154	0.155	0.181	0.185	0.157	0.140	0.144	0.149	0.162	0.228	0.296	0.268
C_{2v}	$^2A_2$	0.059	0.023	0.021	0.003	0.011	0.018	0.007	0.006	0.047	0.027	0.008	0.007	0.023
	$^2B_2$	0.086	0.055	0.054	0.033	0.039	0.054	0.017	0.028	0.090	0.024	0.036	0.028	0.060
	$^2A_1$	0.062	0.063	0.056	0.080	0.053	0.040	0.059	0.054	0.054	0.178	0.071	0.115	0.021
	$^2B_1$	0.250	–[b]	–[b]	0.095	0.120	–[b]	0.135	0.125	0.228	0.169	0.075	0.099	0.083
Mean		0.104	0.081	0.080	0.087	0.089	0.076	0.076	0.076	0.106	0.108	0.085	0.112	0.093
Mean –$^2B_1$[c]		0.075	0.081	0.080	0.086	0.083	0.076	0.064	0.067	0.082	0.096	0.087	0.115	0.094

[a] For the calculation of the STD we have used the distances in an Angstroms and angles in radians. STD values have been calculated as:

$$\left(\frac{\sum_{i=1}^{N} \left(d_i^{\text{Level of theory}} - d_i^{\text{CCSD(T)}} \right)^2}{N} \right)^{\frac{1}{2}}$$

with N=3 ($R_{Cu\text{-}O}$, $R_{O\text{-}O}$, α_{CuOO}).

[b] The SCF process in this state could not be converged.

[c] The results of the $^2B_1$ state are not taking into account in the calculation of the STD.

TABLE 3. Relative Energies (in kcal mol^{-1}) of the Ground and Low-Lying Electronic States of CuO_2 at Different Levels of Theory with the 6-311+G(d) basis set.

symmetry	state	HF	BLYP	G96LYP	OLYP	OPBE	mPWPW91	B3LYP	B3LYP*	BHandH	M05	VSXC	HCTH	TPSS	CCSD(T)
C_s	$^2A''$	0.00	0.00	0.00	0.00	0.00	0.00	0.00	0.00	0.00	0.00	0.00	0.00	0.00	0.03
	$^2A'$	3.77	17.50	17.44	18.26	18.31	17.46	13.41	14.53	8.63	13.05	47.77	18.99	42.85	8.49
C_{2v}	$^2A_2$	1.72	14.83	14.63	15.27	14.49	13.97	8.98	10.27	2.02	8.30	8.01	15.84	10.88	0.00
	$^2B_2$	7.31	19.76	19.48	21.30	20.35	18.79	15.37	16.37	9.46	15.90	15.03	22.57	14.62	7.86
	$^2A_1$	20.57	46.35	46.21	49.39	48.26	45.14	50.30	48.92	56.86	57.55	49.62	53.33	43.40	40.66
	$^2B_1$	81.16	–[b]	–[b]	73.49	75.90	–[b]	77.18	74.71	89.46	85.11	66.35	76.54	64.63	66.93
STD[a]		10.26	9.75	9.59	10.23	10.01	9.11	7.74	7.56	11.38	11.33	17.03	11.76	15.04	–
Mean $-^2B_1$[c]		9.26	9.75	9.59	10.82	10.20	9.11	7.13	7.52	7.34	9.38	18.65	12.15	16.44	–

[a] Standard deviation values have been calculated as:

$$\left(\frac{\sum_{i=1}^{N} \left(E_i^{\text{Level of theory}} - E_i^{\text{CCSD(T)}} \right)^2}{N} \right)^{\frac{1}{2}}$$

with N=6 ($E(^2A'')$, $E(^2A')$, $E(^2A_2)$, $E(^2B_2)$, $E(^2A_1)$, $E(^2B_1)$).

[b] The SCF process in this state could not be converged.

[c] The results of the $^2B_1$ state are not taking into account in the calculation of the STD.

TABLE 4. Relative Energies (in kcal mol^{-1}) of the Ground and Low-Lying Electronic States of CuO_2 at CCSD(T) Level of Theory with different Basis Sets at the optimized CCSD(T)/6-311+G(d) geometry.

symmetry	state	aug-cc-pVTZ	aug-cc-pVQZ	CBS limit
C_s	$^2A''$	1.38	1.38	1.38
	$^2A'$	9.34	9.33	9.33
C_{2v}	$^2A_2$	0.00	0.00	0.00
	$^2B_2$	6.96	6.95	6.94
	$^2A_1$	40.02	40.48	40.82
	$^2B_1$	71.08	73.19	74.73

TABLE 5. Optimized Geometric Parameters of the two lowest-electronic states ($^2A_2$ and ^2A") and relative energy (ΔE, kcal/mol) of the ^2A" with respect to the $^2A_2$ Electronic States of CuO_2 at the CCSD(T) Level of Theory with the aug-cc-pVTZ and aug-cc-pVQZ Basis Sets.

	state	geometry	aug-cc-pVTZ	aug-cc-pVQZ
C_{2v}	$^2A_2$	$R_{Cu\text{-}O}$	1.986	1.982
		$R_{O\text{-}O}$	1.377	1.370
		α_{CuOO}	69.7	69.8
C_s	^2A"	$R_{Cu\text{-}O}{}^b$	1.857	1.854
		$R_{O\text{-}O}$	1.341	1.336
		α_{CuOO}	104.1	103.2
ΔE			1.39	1.38
ΔE (CBS limit)			-	1.38

TABLE 6. Binding dissociation energies (kcal mol^{-1}) of CuO_2 in its the electronic ground state with the 6-311+G(d) basis set for different methods of calculation used.

	HF	BLYP	G96LYP	OLYP	OPBE	mPWPW91	B3LYP	B3LYP*	BHandH	M05	VSXC	HCTH	TPSS	CCSD(T)[a]	CCSD(T)[b]	CCSD(T)[c]	Exp.
BDE (kcal mol^{-1})	-11.11	19.94	17.14	12.53	12.60	19.85	12.74	15.06	11.60	13.09	22.02	14.02	20.90	6.52	13.78	13.81	15±5[d]

[a] 6-311+G(d) basis set.
[b] aug-cc-pVTZ basis set.
[c] aug-cc-pVQZ basis set.
[d] From ref. 36.

TABLE 7. Optimized Geometric Parameters[a] of the Ground and Low-Lying Electronic States of CuO_2 Computed with the B3LYP Method Using Different Parameter Sets[b] with Basis 6-311+G(d).

			Parameter set										
symmetry	state	geometry	0	1	2	3	4	5	6	7	8	9	HF
C_s	$^2A''$	$R_{Cu\text{-}O}$[c]	1.907	1.918	1.920	1.914	1.897	1.889	1.886	1.888	1.890	1.892	1.915
		$R_{O\text{-}O}$	1.303	1.293	1.286	1.285	1.291	1.294	1.293	1.290	1.285	1.280	1.299
		α_{CuOO}	119.6	118.7	117.8	116.8	115.1	113.4	112.0	110.7	109.8	109.5	110.0
	$^2A'$	$R_{Cu\text{-}O}$[c]	1.825	2.013	1.834	1.840	1.846	1.852	1.859	1.865	1.870	1.875	1.900
		$R_{O\text{-}O}$	1.358	1.387	1.345	1.338	1.331	1.322	1.315	1.307	1.298	1.294	1.313
		α_{CuOO}	115.5	114.5	113.9	113.3	112.9	113.0	112.3	112.3	112.5	112.9	113.4
C_{2v}	$^2A_2$	$R_{Cu\text{-}O}$	2.007	2.013	2.018	2.022	2.025	2.029	2.032	2.035	2.039	2.041	2.070
		$R_{O\text{-}O}$	1.412	1.387	1.367	1.351	1.336	1.323	1.312	1.301	1.292	1.283	1.294
		α_{CuOO}	69.4	69.8	70.2	70.5	70.7	71.0	71.2	71.4	71.5	71.7	71.8
	$^2B_2$	$R_{Cu\text{-}O}$	1.925	1.942	1.963	1.984	2.000	2.014	2.027	2.035	2.042	2.049	2.091
		$R_{O\text{-}O}$	1.469	1.433	1.403	1.379	1.360	1.343	1.329	1.318	1.317	1.296	1.308
		α_{CuOO}	67.6	68.3	69.1	69.7	70.1	70.5	70.9	71.1	71.4	71.6	71.8
	$^2A_1$	$R_{Cu\text{-}O}$	2.039	2.037	2.053	2.035	1.997	1.979	1.990	1.986	1.995	1.995	2.036
		$R_{O\text{-}O}$	1.316	1.295	1.286	1.279	1.289	1.300	1.303	1.300	1.295	1.288	1.304
		α_{CuOO}	71.2	71.5	71.8	71.7	71.2	70.9	70.8	70.9	71.0	71.2	71.3
	$^2B_1$	$R_{Cu\text{-}O}$	–[d]	1.889	1.883	1.869	1.845	1.823	1.818	1.802	1.813	1.811	1.830
		$R_{O\text{-}O}$	–[d]	1.764	1.716	1.679	1.640	1.600	1.569	1.545	1.525	1.508	1.522
		α_{CuOO}	–[d]	62.2	62.9	63.3	63.6	64.0	64.4	64.8	65.1	65.4	65.4

[a] Distances are in angstroms and angles in degrees.
[b] See Table S1.
[c] Cu–O bond length corresponding to the shortest Cu–O distance.
[d] This state can not be converged with the BLYP functional (set 0).

TABLE 8. Calculation of the STD of the Geometric Parameters of the Ground and Low-Lying Electronic States of CuO_2 Computed with the B3LYP Method Using Different Parameter Sets[a] with Basis 6-311+G(d).

		Parameter set										
symmetry	state	0	1	2	3	4	5	6	7	8	9	HF
C_s	$^2A''$	0.110	0.104	0.097	0.086	0.068	0.050	0.039	0.030	0.028	0.031	0.030
	$^2A'$	0.154	0.321	0.138	0.132	0.129	0.131	0.125	0.127	0.131	0.135	0.139
C_{2v}	$^2A_2$	0.023	0.008	0.005	0.015	0.024	0.032	0.039	0.046	0.052	0.057	0.059
	$^2B_2$	0.055	0.032	0.011	0.012	0.026	0.039	0.050	0.059	0.074	0.074	0.086
	$^2A_1$	0.063	0.064	0.075	0.066	0.042	0.030	0.035	0.034	0.040	0.042	0.062
	$^2B_1$	–[b,c]	0.103	0.131	0.154	0.179	0.205	0.223	0.239	0.249	0.259	0.250
Mean		0.081	0.105	0.076	0.077	0.078	0.081	0.085	0.089	0.096	0.100	0.104
Mean $-^2B_1$[c]		0.081	0.126	0.091	0.093	0.094	0.097	0.102	0.107	0.115	0.120	0.125

[a] See Table S1.
[b] This state cannot be converged with the BLYP functional (set 0).
[c] The results of the $^2B_1$ state are not taking into account in the calculation of the STD.

TABLE 9: Relative Energies (in kcal mol^{-1}) of the Ground and Low-Lying Electronic States of CuO_2 Computed with the B3LYP Method Using Different Parameter Sets[a] with Basis 6-311+G(d).

		Parameter set										
symmetry	state	0	1	2	3	4	5	6	7	8	9	HF
C_s	$^2A''$	0.00	0.00	0.00	0.00	0.00	0.00	0.00	0.00	0.00	0.00	0.00
	$^2A'$	17.50	15.41	13.25	11.07	9.11	7.60	6.50	5.66	5.02	4.50	3.77
C_{2v}	$^2A_2$	14.83	11.80	9.04	6.52	4.43	2.95	1.98	1.36	0.98	0.78	1.72
	$^2B_2$	19.76	17.57	15.41	13.18	11.14	9.57	8.44	7.63	7.14	6.67	7.31
	$^2A_1$	46.35	48.09	50.33	51.89	52.78	52.32	50.50	47.93	45.08	42.20	20.57
	$^2B_1$	–[b]	71.46	76.89	82.17	87.13	90.49	91.38	90.94	89.90	88.55	81.16
Mean[c]		9.75	7.72	7.68	8.52	9.88	10.83	10.82	10.32	9.67	9.02	10.26
Mean $-^2B_1$[d]		9.75	8.21	7.14	6.38	5.96	5.45	4.58	3.54	2.57	2.02	9.26

[a] See Table S1.

[b] This state cannot be converged with the BLYP functional.

[c] Standard deviation values have been calculated as:

$$\left(\frac{\sum_{i=1}^{N} \left(E_i^{\text{Level of theory}} - E_i^{\text{CCSD(T)}} \right)^2}{N} \right)^{\frac{1}{2}}$$

with N=6 ($E(^2A'')$, $E(^2A')$, $E(^2A_2)$, $E(^2B_2)$, $E(^2A_1)$, $E(^2B_1)$). CCSD(T) relative energies used are those of Table 3.

[d] The results of the $^2B_1$ state are not taking into account in the calculation of the STD.

TABLE 10. Number of imaginary frequencies of the C_{2v} and C_s stationary points for the ground state and low-lying electronic states considering the different methods used.

symmetry	state	HF	G96LYP	OLYP	OPBE	mPWPW91	B3LYP	B3LYP*	BHandH	M05	VSXC	HCTH	TPSS	CCSD(T)
C_s	$^2A''$	0	0	0	0	0	0	0	0	0	0	0	0	0
	$^2A'$	0	0	0	0	0	0	0	0	0	0	0	0	0
C_{2v}	$^2A_2$	1	1	1	1	1	1	1	0	1	0	1	1	0
	$^2B_2$	1	0	0	0	0	0	0	0	0	0	0	0	0
	$^2A_1$	1	0	0	0	0	0	0	0	0	0	0	0	–[a]
	$^2B_1$	0	0	0	0	0	0	0	0	0	0	0	0	–[a]

[a] Calculations for these states are not possible because the numerical procedure breaks the symmetry of the molecule.

symmetry	state	B3LYP									
		0	1	2	3	4	5	6	7	8	9
C_s	$^2A''$	0	0	0	0	0	0	0	0	0	0
	$^2A'$	0	0	0	0	0	0	0	0	0	0
C_{2v}	$^2A_2$	1	1	1	1	1	1	0	0	0	0
	$^2B_2$	0	0	0	0	1	1	1	1	1	1
	$^2A_1$	0	0	0	0	0	0	0	0	1	1
	$^2B_1$	0	0	0	0	0	0	0	0	0	0